© 2020. Published by The Company of Biologists Ltd | Journal of Experimental Biology (2020) 223, jeb233197. doi:10.1242/jeb.233197

RESEARCH ARTICLE

Cytoskeletal and synaptic polarity of LWamide-like+ ganglion neurons in the sea anemone *Nematostella vectensis*

Michelle C. Stone[1], Gregory O. Kothe[1], Melissa M. Rolls[1,*] and Timothy Jegla[2,*]

ABSTRACT

The centralized nervous systems of bilaterian animals rely on directional signaling facilitated by polarized neurons with specialized axons and dendrites. It is not known whether axo-dendritic polarity is exclusive to bilaterians or was already present in early metazoans. We therefore examined neurite polarity in the starlet sea anemone *Nematostella vectensis* (Cnidaria). Cnidarians form a sister clade to bilaterians and share many neuronal building blocks characteristic of bilaterians, including channels, receptors and synaptic proteins, but their nervous systems comprise a comparatively simple net distributed throughout the body. We developed a tool kit of fluorescent polarity markers for live imaging analysis of polarity in an identified neuron type, large ganglion cells of the body column nerve net that express the LWamide-like neuropeptide. Microtubule polarity differs in bilaterian axons and dendrites, and this in part underlies polarized distribution of cargo to the two types of processes. However, in LWamide-like+ neurons, all neurites had axon-like microtubule polarity suggesting that they may have similar contents. Indeed, presynaptic and postsynaptic markers trafficked to all neurites and accumulated at varicosities where neurites from different neurons often crossed, suggesting the presence of bidirectional synaptic contacts. Furthermore, we could not identify a diffusion barrier in the plasma membrane of any of the neurites like the axon initial segment barrier that separates the axonal and somatodendritic compartments in bilaterian neurons. We conclude that at least one type of neuron in *Nematostella vectensis* lacks the axo-dendritic polarity characteristic of bilaterian neurons.

KEY WORDS: *Nematostella*, Cnidarian, Neuronal polarity, Axon, Dendrite

INTRODUCTION

Neuronal polarity at the cellular level is a fundamental feature of centralized bilaterian nervous systems. These nervous systems rely on individual neurons to send directional signals within complex circuits necessary for information processing and behavior. The polarized neuron has evolved to accomplish this task by specialization of neuronal processes into axons to send signals and dendrites to receive them. Differences in the distribution of cellular components underlie this functional specialization. For example, mitochondria and smooth endoplasmic reticulum are present throughout the neuron. Golgi outposts and ribosomes are found in dendrites and are much less abundant in axons (Bartlett and Banker, 1984; Craig and Banker, 1994). Similarly, presynaptic machinery is typically found in the axon and postsynaptic machinery in the dendrites, although some exceptions such as axo-axonal and dendro-dendritic synapses exist (Inan et al., 2013; Ren et al., 2007; Strowbridge, 2009). Polarized trafficking is believed to play a role in the differential distribution of proteins and organelles to axons and dendrites, and vertebrate axons and dendrites do indeed fundamentally differ in the arrangement of their microtubule cytoskeleton. Microtubules in the axon are organized in a plus end-out array, meaning that the more dynamic plus ends are all oriented away from the cell body (Baas and Lin, 2011). In contrast, dendrites of rodent neurons *in vitro* (Baas et al., 1988) and *in vivo* (Yau et al., 2016) and adult frog mitral cells (Burton, 1988) have mixed polarity microtubule arrays. This difference in microtubule polarity between axons and dendrites can be used to direct cargoes from the primary site of synthesis in the cell body to a specific destination. For example, the minus end-directed motor dynein can transport cargoes including AMPA receptors into dendrites, but not axons, based on polarity of microtubule tracks (Kapitein et al., 2010).

Initially, it was thought that axo-dendritic neuronal polarity was a characteristic specific to vertebrate neurons as many invertebrate neurons are unipolar with a single primary neurite extending from the cell body (Craig and Banker, 1994). However, recent studies have provided strong evidence that key features of axons and dendrites are conserved across the Bilateria. In *Drosophila* neurons, many key features of polarized neurons have been described including (1) pre- and postsynaptic segregation, and (2) localization of protein synthetic machinery including ribosomes and Golgi selectively to dendrites (Rolls, 2011; Rolls and Jegla, 2015). Microtubule polarity also distinguishes axons and dendrites across multiple bilaterian invertebrate neuron types. *Drosophila* multipolar sensory neurons have axons with an all plus-end-out microtubule array while dendrites have a greater than 90% minus-end-out arrangement (Rolls et al., 2007; Stone et al., 2008). Furthermore, in unipolar motor and interneurons, the primary neurite branches into an axon with a plus end-out microtubule array and a dendrite with a minus end-out microtubule array (Stone et al., 2008). In the nematode *C. elegans*, similar findings were reported for axons and dendrites of motor neurons, with axons being plus end-out and dendrites minus end-out (Goodwin et al., 2012), and similar organization is found in a variety of other neuron types (Harterink et al., 2018). The difference in microtubule polarity between axons and dendrites is a likely contributor to the differentiation between the two compartments. Indeed, the genetic removal of minus end-out microtubules from dendrites in both mammals and *C. elegans* resulted in the loss of dendrite-specific markers and dendrites becoming more axon-like (Lin et al., 2012; Sharp et al., 1997; Yan et al., 2013). Thus, in the bilaterian species so far examined, the

[1]Department of Biochemistry and Molecular Biology and the Huck Institutes of the Life Sciences, The Pennsylvania State University, University Park, PA 16802, USA. [2]Department of Biology and the Huck Institutes of the Life Sciences, The Pennsylvania State University, University Park, PA 16802, USA.

*Authors for correspondence (mur22@psu.edu; tjj3@psu.edu)

M.M.R., 0000-0002-5021-4360; T.J., 0000-0001-8616-2390

Received 13 July 2020; Accepted 14 September 2020

Journal of Experimental Biology (2020) 223, jeb233197. doi:10.1242/jeb.233197

presence of minus-end-out microtubules is closely associated with dendrite identity.

Another feature of polarized neurons that helps direct the positioning of axon- or dendrite-specific components is the axon initial segment (AIS). In many vertebrate neurons, the region of the axon just past the cell body is the site of action potential initiation (Bender and Trussell, 2012) and has a specialized cytoskeleton to anchor voltage-gated ion channels required for action potential initiation and regulation (Dodson et al., 2002; Goldberg et al., 2008; Johnston et al., 2008; Lorincz and Nusser, 2008; Pan et al., 2006; Rasband et al., 1998; Sarmiere et al., 2008; Shah et al., 2008). The unique cytoskeletal organization of the AIS also provides a plasma membrane diffusion barrier for lipids and proteins to separate the axonal and somatodendritic membranes (Kobayashi et al., 1992; Winckler et al., 1999). Ankyrin G (AnkG) localizes to the AIS of vertebrate neurons (Kordeli et al., 1995) and is a key component of the AIS cytoskeletal scaffold. AnkG binds to B-IV-spectrin, which in turn binds to the actin cytoskeleton, creating a barrier against certain lipids and proteins not destined for the axon (Berghs et al., 2000; Grubb and Burrone, 2010; Leterrier and Dargent, 2014). AnkG is vertebrate specific and therefore the existence of an AIS outside of vertebrate neurons was in question (Jenkins et al., 2015) until studies in *Drosophila* revealed that an orthologous giant ankyrin (Ank2) is required for a plasma membrane diffusion barrier in the proximal axon of multipolar sensory neurons (Jegla et al., 2016). Thus at least some functional features of a giant ankyrin-based AIS are evolutionarily conserved among bilaterians.

The question we begin to address here is whether axo-dendritic neuronal polarity is found beyond bilaterians. Genome analyses place cnidarians (sea anemones, jellyfish and corals for example) as a sister clade to bilaterians (Ryan et al., 2010, 2013; Srivastava et al., 2008) (Fig. 1). Cnidarians are thus in a unique position to provide insight into the evolutionary origin of axo-dendritic neuronal polarity and whether it predates centralization of the nervous system in bilaterians. Limited centralization can occur in the swimming adult medusae of some jellyfish species, though it is thought to have evolved independently in these medusozoan lineages (Mackie, 2004; Satterlie, 2011). The nervous system of cnidarian polyps, the most widespread cnidarian body morphology, takes the form of a net without bilaterian-style centralization (Nakanishi et al., 2012). This polyp nerve net morphology is believed to be ancestral in cnidarians (Mackie, 2004; Watanabe et al., 2009) and is retained in the anthozoans (sea anemones and corals) for which the polyp is the adult body form. Despite their simplicity, cnidarian nerve nets comprise multiple functional classes of neurons as well as cnidocytes and stinging cells unique to cnidarians that share a developmental lineage with neurons (Dupre and Yuste, 2017; Marlow et al., 2009; Nakanishi et al., 2012; Rentzsch et al., 2019; Sebe-Pedros et al., 2018). Recent whole organism single-cell RNAseq analysis distinguishes up to 32 neuronal cell types in a sea anemone larvae and polyps (Sebe-Pedros et al., 2018), suggesting that cell type diversity within the nerve net is broader than previously appreciated.

It is currently unknown whether any of these diverse cnidarian neurons display functional polarity in terms of cellular structure, and thus whether they have a true axon or dendrites comparable to those seen in bilaterians. One argument against the existence of neuronal polarity in cnidarians comes from the observation of bidirectional synapses in jellyfish and hydra (Anderson, 1985; Anderson and Grünert, 1988; Horridge et al., 1962; Kinnamon and Westfall, 1982) although polarized chemical synapses have also been reported (Anderson and Spencer, 1989). In contrast, sequence

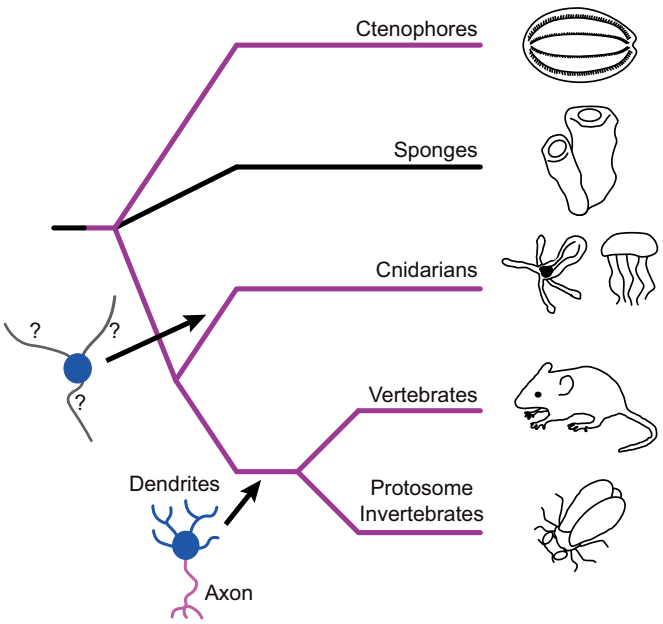

Fig. 1. Schematic phylogeny of major metazoan lineages based on genome sequences. Purple lines indicate lineages containing nervous systems. The nervous system evolved early in the evolutionary history of metazoans, but the divergence order of sponges and ctenophores is contentious. It is therefore unclear if the nervous system predates radiation of all extant metazoans as depicted here (and was lost in sponges), evolved after the divergence of sponges or evolved independently in the ctenophore lineage (Ryan, 2014). Functionally polarized neurons with distinct axons (magenta) and dendrites (blue) are characteristic of bilaterians and have been well characterized at the cellular level in both deuterostome and protostome invertebrate model organisms. Cnidarians form a sister group to the bilaterians, but the functional polarity of their neurites has not been examined on a molecular level. It is therefore unknown if true axons and dendrites predate the cnidarian/bilaterian divergence.

data from *Nematostella vectensis* and *Hydra magnipapillata* revealed orthologs for most neuronal signaling proteins found in bilaterians (Chapman et al., 2010; Putnam et al., 2007). In addition, almost all major classes of voltage-gated ion channels found in bilatarian axons and dendrites are conserved in cnidarians (Baker et al., 2015; Gur Barzilai et al., 2012; Jegla et al., 1995, 2012, 2009; Jegla and Salkoff, 1997; Li et al., 2015a,b; Martinson et al., 2014; Moran et al., 2015; Moran and Zakon, 2014). Finally, B-spectrin and ankyrin, two key components of the AIS scaffold, have been shown to be present in cnidarians (Bennett and Lorenzo, 2013; Jegla et al., 2016). However, giant ankyrin isoforms required for AIS formation in bilaterians appear to be absent in cnidarians (Jegla et al., 2016). Thus many, but not all, of the known building blocks used to make polarized neurons are present in cnidarians.

Here we used the starlet sea anemone *Nematostella vectensis* Stephenson 1935 as a model system for studying neuronal polarity in cnidarians. *Nematostella* has been extensively used to examine evolutionary conservation of neuronal development (Kelava et al., 2015; Layden et al., 2012, 2016b; Layden and Martindale, 2014; Marlow et al., 2009; Nakanishi et al., 2012). It has a sequenced and annotated genome (Putnam et al., 2007) and is relatively easy and inexpensive to maintain in culture (Fritzenwanker and Technau, 2002; Hand and Uhlinger, 1992; Stefanik et al., 2013). In addition, genetic manipulation can be achieved through microinjection of embryos (Layden et al., 2013). Thus, *Nematostella* is a good system to examine neuronal polarity in cnidarians. Here we developed fluorescent tools to examine microtubule polarity, diffusion barriers

Journal of Experimental Biology (2020) 223, jeb233197. doi:10.1242/jeb.233197

and synaptic arrangements in LWamide-like+ bipolar and tripolar ganglion neurons that span the body column of *Nematostella* (Havrilak et al., 2017). LWamide-like+ ganglion neurons in *Nematostella* have long, largely unbranched neurites emanating from isolated cell bodies that extend throughout the body wall of the animal (Layden et al., 2016b). We chose this cell type for initial analysis because its low density facilitates analysis of single cells in live animals and the LWamide-like peptide is expressed in only three of the 32 potential neuronal cell types identified by whole organism transcriptional profiling (Sebe-Pedros et al., 2018), indicating that they represent a relatively homogenous population of neurons. Furthermore, anatomically similar ganglion neurons have been observed in diverse medusozoans (Anderson, 1985; Dupre and Yuste, 2017; Norekian and Moroz, 2020) and LWamide-like peptide precursors are found in diverse cnidarians (Gajewski et al., 1996; Mitgutsch et al., 1999; Nielsen et al., 2019; Plickert et al., 2003), suggesting that they could represent a conserved type of cnidarian neuron. We find that all neurites of LWamide-like+ ganglion neurons have axon-like microtubule polarity but lack plasma membrane diffusion barriers and appear to connect at least in part via bidirectional chemical synapses.

MATERIALS AND METHODS

Molecular cloning

Annotated sequences of all plasmids used in this study are included in Dataset 1 and all transgenic constructs are described in Fig. 2. We used a previously-described Sce-I meganuclease-based strategy to insert transgenes into *Nematostella* (Renfer et al., 2010). Briefly, we used a PCR to insert two Sce-I meganuclease sites surrounding a polylinker followed by an SV40 polyadenylation sequence into the expression vector plasmid pOX (Jegla and Salkoff, 1997) to create a carrier plasmid (NvT, see sequence in Dataset 1) for transgene markers. Excision of the transgene with Sce-I prior to embryo injection facilitates transgene integration and expression (Renfer et al., 2010). *Nematostella* EB1 (NvEB1, XM_032367625), Synaptobrevin (NvSynaptobrevin, XM_001634396) and Homer (NvHomer, XM_032362162) were cloned from polyp mRNA by RT-PCR and the NvLWamide-like neuropeptide precursor was PCR cloned from *Nematostella* genomic DNA. Coding sequence for all four *Nematostella* peptides was then fused to fluorescent markers as described in Fig. 2 using overlap PCR. The open reading frames of all reporter constructs were verified by sequencing after cloning. The NvLWamide-like (Havrilak et al., 2017) and NvElav1 promoters (Nakanishi et al., 2012) were cloned by PCR from genomic DNA and end sequenced to confirm fragment identity after cloning. For some constructs, the primary marker protein's ORF was followed by an in frame *Thosea asigna* virus 2A sequence (Daniels et al., 2014) and mCherry (Shu et al., 2006) to allow us to express both the neuronal marker (NvEB1-eGFP for example) and mCherry as separate peptides from a single ORF. The separate cytoplasmic mCherry marker aided screening for transgenic animals at low magnification because of lower background fluoresence in the red channel. For co-expression of NvElav1::NvSynaptobrevin-mCherry and NvLWamide-like::NvHomer-eGFP, the two individual expression cassettes were combined in a single plasmid via Infusion cloning (Takara Bio, cat. no. 638911). In this construct, the NvLWamide-like::NvHomer-eGFP cassette lacked a dedicated polyadenylation signal after the stop codon, but expression was nevertheless robust.

Sea anemone care and spawning

Nematostella were housed in soda lime glass bowls (Carolina Biological cat. no. 741006) in 12 g l^{-1} Instant Ocean (Carolina Biological, cat. no. 671442) and fed a diet of Artemia (Brine Shrimp Direct, cat. no. BSEA8Z). Animals were maintained in the dark at room temperature. Adults >6 months in age were used for spawning and females were maintained in separate bowls to allow for controlled fertilization. Spawning was initiated with an 8–10 h light exposure using a standard fluorescent light box. The light box raised water temperature to ∼30°C and robust spawning required both light and heat. Egg sacs from all female bowls were isolated and mixed with water from bowls containing males within 1 h of spawning for synchronous fertilization. Following a 15–30 min incubation, fertilized embryos were isolated from egg sacs using gentle agitation in Instant Ocean (12 g l^{-1}) supplemented with 2% L-cysteine (Sigma-Aldrich, VWR, cat. no. C7352) and adjusted to pH 8.5 with NaOH (Sigma-Aldrich, cat. no. SX0607N). Embryos were rinsed 3–5 times in 12 g l^{-1} Instant Ocean to remove the cysteine and immediately moved to Falcon 353007 60 mm polystyrene dishes (VWR, cat. no. 25373-085) for microinjection. Embryos adhered to the dish for several hours, facilitating injection.

Embryo injection and identification of transgenic polyps

Needles for embryo injection were pulled from 1 mm thin-walled borosilicate glass capillaries (BF100-78, Sutter Instruments) using a P-1000 Micropipette Puller (Sutter Instruments) and filled by capillary action. Injection mixes included the targeting plasmid at 40 ng μl^{-1}, 1× CutSmart® Buffer (New England Biolabs, cat. no. B7204S), 5 units SceI meganuclease (New England Biolabs, cat. no. R0694S) used to release transgenic promoter-reporter constructs from the parent plasmid and 100 µmol l^{-1} Alexa-Fluor 488 or 568 (Thermo Fisher, cat. no. D22910, D22912) to mark injected embryos. Mixes were incubated 1 h at 37°C prior to needle loading. Injections were carried out using a Femtojet injector (Eppendorf) and a MO-202U Joystick manipulator (Narashige) mounted on a MMN-1 course manipulator (Narashige). A Zeiss Axio Zoom.v16 with standard GFP/RFP filter cubes coupled to a HXP 200C metal halide illuminator (Zeiss) was used for embryo visualization during injection. We did not quantify injection volume, but for each needle we optimized the injection time and pressure to achieve the maximum injection volume that did not physically damage the embryos. The injection room was held at 16–18°C to slow embryo cleavage. Embryos were injected at the single cell stage and hundreds of embryos could typically be injected prior to the onset of cell divisions.

Animals were screened for expression of transgenes (detected by presence of fluorescent markers in neurons) after development into 4 tentacle polyps (1–2 weeks) using the Axio Zoom.v16 scope and GFP or RFP filters. Fluorescent dyes used to mark embryos during injection were no longer detectable at this stage and thus did not complicate the screening process. Most polyps were mosaic transgenics with <20 labeled neurons. Low numbers of labeled neurons facilitated identification of neurites extending from cells of interest during subsequent imaging experiments. For typical injection sessions, approximately 10–30% of the polyps showed transgene expression in at least some neurons.

Live imaging of *Nematostella*

Whole, live *Nematostella* polyps at the 4–6 tentacle stage were anesthetized in 12 g l^{-1} Instant Ocean supplemented with 2% urethane (Sigma-Aldrich cat. no. U2500) until tentacles were completely extended. They were then mounted for imaging using a method we developed for optimization of animal stillness, image quality and viability of the polyps. This mounting method consisted of a metal slide with a 12 mm diameter hole in the center. The

Journal of Experimental Biology (2020) 223, jeb233197. doi:10.1242/jeb.233197

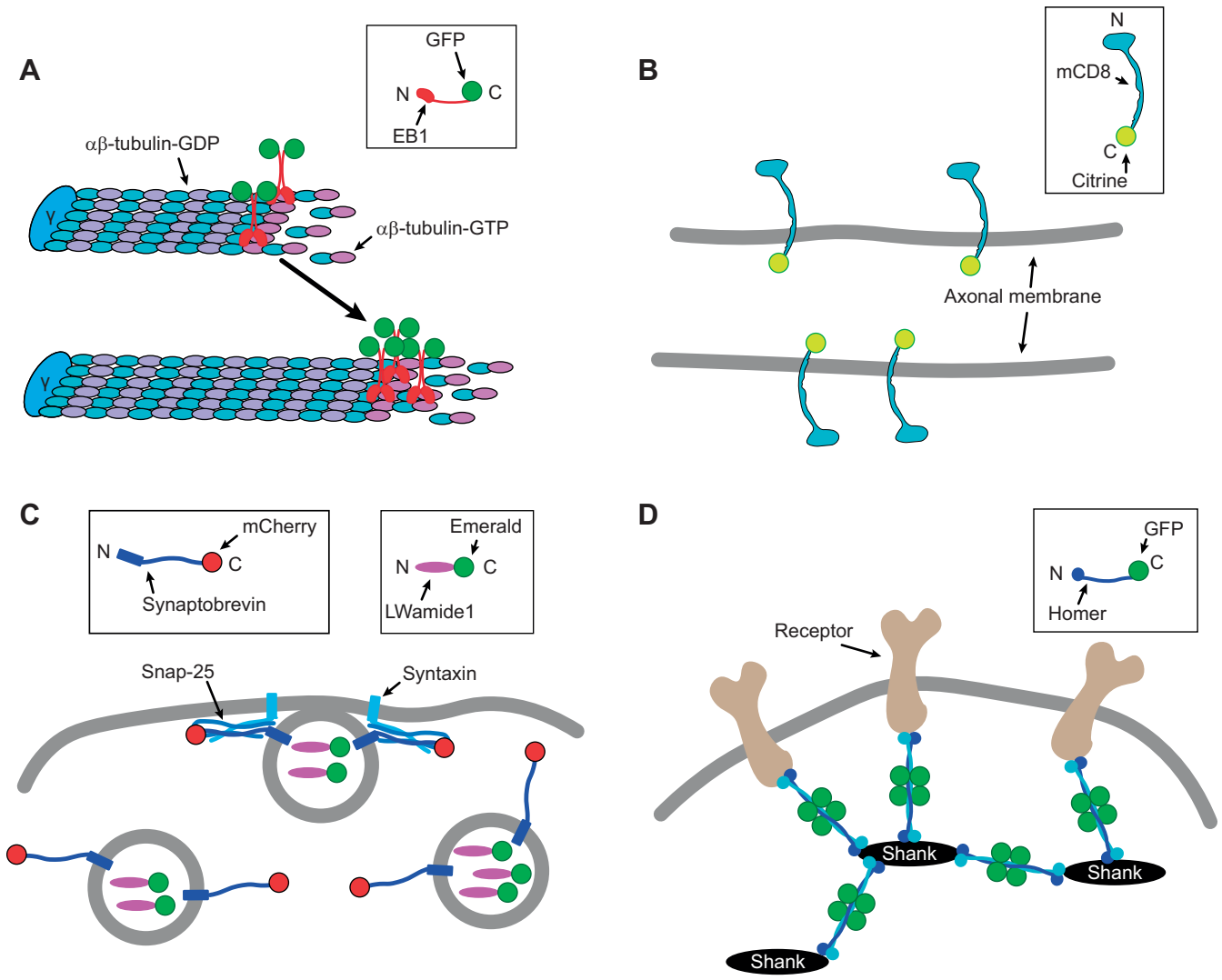

Fig. 2. Marker proteins used to examine polarity in LWamide-like+ *Nematostella* neurons. (A) C-terminal fusion of GFP to NvEB1 labels the plus end of microtubules in the GTP-tubulin cap region. The γ-tubulin ring complex (γ) nucleates microtubules and can cap the minus end. This region moves over time as microtubules polymerize (arrow). (B) C-terminal fusion of Citrine to mCD8 makes a transmembrane fluorescent marker labeled on the cytoplasmic side. The marker is not tethered and can diffuse in the plane of the membrane. (C) C-terminal fusion of mCherry to NvSynaptobrevin, the synaptic vesicle SNARE protein and Emerald to the LWamide-like peptide precursor label synaptic vesicles to mark presynaptic release sites. (D) C-terminal fusion of GFP to NvHomer labels the postsynaptic scaffold network formed by Homer and Shank. The identity of receptor targets of Homer at *Nematostella* synapses is unknown.

underside opening in the slide was covered with an air permeable membrane (VWR, cat. no. 52457-563) and held in place by tape. The top side of the opening was covered with a piece of nylon mesh (Genesee Scientific, cat. no. 57-102) The nylon mesh was pulled tightly across the opening to create a sturdy, solid surface and held in place with super glue. Polyps were then mounted on top of the nylon mesh in a droplet of 12 g l^{-1} Instant Ocean supplemented with 2% urethane. Finally, the polyp was covered with a 12 mm round coverslip (VWR, cat. no. 89015-725), which was secured into place with tape over the opening of the slide. The coverslip lightly presses the polyp against the mesh hammock over the hole in the slide, and the liquid is kept in place by the lower membrane (see Fig. 3A). The combination of urethane anesthesia and light physical pressure reduced movement sufficiently to enable temporal imaging.

For microtubule polarity analysis, neurons were imaged on a Zeiss upright LSM 800 confocal microscope. NvEB1-GFP videos were acquired using a 63× 1.4 NA oil immersion objective and captured at 1 frame per 0.93 or 1.27 s. Videos were analyzed using ImageJ software (https://imagej.nih.gov/ij/) by tracking the movement of NvEB1-GFP comets either towards or away from the cell body. Only comets that were visible in three consecutive frames were scored.

For longitudinal imaging of potential microtubule organizing centers (MTOCs), polyps at the 4–6 tentacle stage were chosen and the first day they were imaged was designated as D0. After imaging at D0, polyps were recovered and returned to 12 g l^{-1} Instant Ocean. They were then reimaged 5 days later (D5). Because *Nematostella* exhibit radial symmetry it was necessary to develop a method to image the polyps in the same orientation in multiple sessions to facilitate tracking of the same neuron. To do this, before mounting on D0 two tentacles were cut off. The polyp was then mounted with the remaining tentacles either up or down and the position was noted in order to remount in the same orientation at D5. This way the same neuron could be found based on morphology and position in relation to other neurons within the animal. Polyps were imaged on a Zeiss upright LSM 800 confocal microscope using a 63× 1.4 NA oil immersion objective.

Journal of Experimental Biology (2020) 223, jeb233197. doi:10.1242/jeb.233197

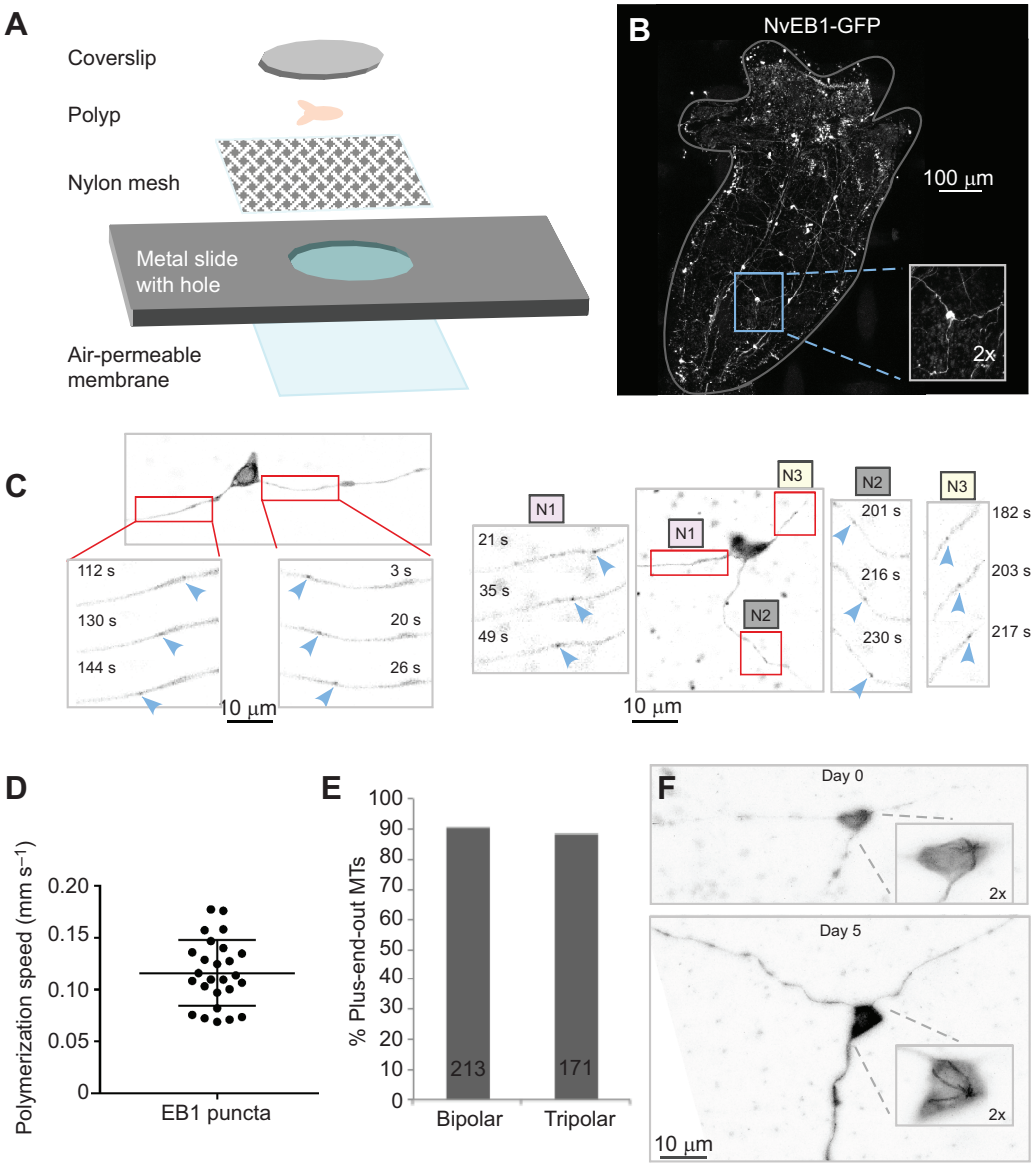

Fig. 3. Microtubule polarity in all neurites of bipolar and tripolar LWamide-like+ ganglion neurons is plus-end out. (A) A diagram showing construction of the live imaging chamber is shown. An air-permeable membrane is attached to the underside of a metal slide with a hole in it. Nylon mesh is glued to the top side of the slide. Polyps are placed in a drop of liquid on the nylon mesh and held in place with a coverslip taped to the top surface of the slide. (B) Whole animal image of a four-tentacle stage polyp expressing NvLWamide-like::NvEB1-GFP. Inset shows example tripolar ganglion neuron within the context of the animal. (C) Representative images of bipolar and tripolar LWamide-like+ ganglion neurons expressing NvLWamide-like::NvEB1-GFP. Insets show NvEB1 puncta moving away from cell body as indicated by blue arrowheads. In the tripolar example N1, N2 and N3 represent neurite 1, neurite 2 and neurite 3, respectively. (D) Quantification of speed of NvEB1 puncta. Points on graph represent the speed of 26 different NvEB1 puncta recorded from 8 tripolar ganglion neurons. Error bars represent s.d. (E) Quantification of direction of NvEB1 puncta in bipolar and tripolar ganglion neurons. Number of puncta analyzed is shown on bar for each type of neuron. (F) Longitudinal imaging of potential MTOC in the cell body of a tripolar LWamide-like+ ganglion neuron expressing NvLWamide-like::NvEB1-GFP. Inset shows the potential MTOC at day 0 and day 5. Cells were identified based on position in the animal relative to a tentacle clipped at day 0. The shape of the cell body can appear slightly different based on how the animal is compressed during mounting.

To test for the presence of a diffusion barrier in tripolar neurons, 5 µm segments of all three neurites were photobleached in regions 0–10 µm, 10–20 µm or 30–100 µm from the cell body in live juvenile polyps at the 4–6 tentacle stage. Fluorescence recovery after photobleaching (FRAP) was analyzed using the FRAP Calculator macro in ImageJ that was developed by Dr Robert Bagnell.

Imaging of pre and postsynaptic markers was done with a Zeiss upright LSM 800 confocal microscope or Zeiss inverted LSM 800 confocal microscope using a 63× 1.4 NA oil immersion objective. Representative images were made by taking max *Z* projections using ImageJ software. In instances where there was a lot of movement in the videos, recursive alignment was done using the StackReg plugin (https://imagej.net/StackReg).

RESULTS

Neuronal marker proteins

To determine the cellular polarity of LWamide-like+ ganglion neurons, we developed markers for examining the polarity of microtubules in the neurites, neurite diffusion barriers and localization of presynaptic and postsynaptic compartments (Fig. 2). To examine microtubule polarity, we utilized a plus end tracking method that was originally developed in cultured neurons

Journal of Experimental Biology (2020) 223, jeb233197. doi:10.1242/jeb.233197

(Stepanova et al., 2003) and has since been used to map microtubule polarity in *Drosophila*, *C. elegans* and rodent neurons *in vivo* (Goodwin et al., 2012; Rolls et al., 2007; Stone et al., 2008; Yau et al., 2016). EB family members including EB1 are +TIP proteins that associate dynamically with growing microtubule ends (Galjart, 2010; Jiang and Akhmanova, 2011). When fluorescently tagged, the direction of EB growth can be used to infer microtubule polarity in neurites (Stepanova et al., 2003). *Nematostella* has a single EB1 ortholog that has previously been used to visualize spindle microtubules during embryo development (DuBuc et al., 2014), but has not been demonstrated to track growing plus ends of microtubules. We fused GFP to the C-terminus of NvEB1 to copy the strategy used for microtubule tracking with bilaterian EB proteins (Fig. 2A).

To label the plasma membrane for visualization of cell shape and to assay diffusion in the plane of the membrane, we fused the mouse transmembrane protein CD8 (mCD8) to the GFP variant Citrine (Griesbeck et al., 2001) (Fig. 2B). mCD8 has been used in *Drosophila* to label the plasma membrane neuronal processes (Lee and Luo, 1999) and because it is a diffusible plasma membrane marker, it has also been used in *Drosophila* to identify a diffusion barrier in axons of cultured neurons (Katsuki et al., 2009). In addition, we have previously used this marker to identify a diffusion barrier in the proximal axon of *Drosophila* sensory neurons *in vivo* (Jegla et al., 2016).

We chose the synaptic vesicle V-SNARE protein Synaptobrevin as a presynaptic marker (Fig. 2C) because Synaptobrevin-GFP fusions localize to the presynaptic compartment in bilaterians (Estes et al., 2000; Nonet, 1999). We found four genes encoding V-SNAREs in the *Nematostella* genome (Putnam et al., 2007) with BLAST searches, but phylogenetic analyses indicated that only one, called NvSynaptobrevin here, is an ortholog of bilaterian Synaptobrevins (Fig. S1, Dataset 2). We therefore reasoned that NvSynaptobrevin would be present at all chemical synapses. As an alternative presynaptic marker, we fused the *Nematostella* neuropeptide LWamide-like precursor to the GFP variant Emerald (Tsien, 1998) (Fig. 2C). The neuropeptide rat atrial natriuretic factor (ANF) fused to Emerald has been used to visualize secretory vesicle localization in cultured mammalian neurons (Han et al., 1999) and at the *Drosophila* larval neuromuscular junction (NMJ) (Rao et al., 2001). Neuropeptide-containing dense core vesicles are assembled in the Golgi complex in the neuronal cell body (Cameron et al., 1993) and are captured at synapses, including en passant synapses (Wong et al., 2012). Their large size compared with small locally generated synaptic vesicles makes them particularly attractive for live imaging of presynaptic components.

Nematostella has a high diversity of channels and receptors (Jegla et al., 2012, 2009; Li et al., 2015a,b; Liebeskind et al., 2015) complicating their use as postsynaptic markers. We therefore focused on receptor scaffolding molecules Homer and DLG as potential postsynaptic markers because *Nematostella* has only a single ortholog of each (Burkhardt et al., 2014; Putnam et al., 2007). Homer proteins have a unique domain structure (Fig. S1A) making their identification unambiguous (Burkhardt et al., 2014). Postsynaptic densities have been visualized in bidirectional cnidarian chemical synapses in scanning electron micrographs (Anderson and Grünert, 1988; Anderson and Spencer, 1989). We did not consistently detect fluorescence of NvDLG-GFP in animals, and therefore used NvHomer-GFP as a postsynaptic marker for LWamide-like+ neurons (Fig. 2D). Homer proteins form a scaffold network in conjunction with Shank that helps cluster receptors and signaling proteins including metabotropic glutamate receptors to the postsynaptic density in bilaterian neurons (Hayashi et al., 2009; Shiraishi-Yamaguchi and Furuichi, 2007). The Homer family comprises three genes in mammals: Homer1, Homer2 and Homer3 (Brakeman et al., 1997; Xiao et al., 1998). In *Drosophila*, there is a single Homer gene that is highly homologous to the mammalian Homer1 protein and Homer-GFP (C-terminal fusion) and has been used as a marker for postsynapses (Diagana et al., 2002; Rolls et al., 2007). Furthermore, a recent study shows that an NvHomer-mCherry fusion appears to label the postsynaptic side of the neuromuscular junction in *Nematostella* (Cole et al., 2020 preprint).

Microtubule polarity in bipolar and tripolar LWamide-like+ ganglion neurons is plus-end-out in all neurites

To determine whether each of the two or three neurites that projected from LWamide-like+ neurons could be distinguished from one another based on microtubule polarity, we drove expression of NvEB1-GFP in LWamide-like+ neurons using a previously characterized LWamide-like promoter fragment (Layden et al., 2016a) and made mosaic NvLWamide-like::NvEB1GFP polyps via embryo injection using an adaptation of a previously described protocol (Layden et al., 2013). To facilitate identification of mosaic animals, we included mCherry downstream of a T2A cleavage site to provide a general cytoplasmic marker to highlight transgenic cells. We found expression of both NvEB1-GFP and mCherry in bipolar and tripolar ganglion neurons, consistent with previous characterizations of LWamide-like+ neurons (Havrilak et al., 2017; Layden et al., 2016a). In order to perform live imaging of growing microtubule plus ends labeled with NvEB1-GFP, we developed a live imaging strategy suitable for small polyps (Fig. 3A). Animals were partially immobilized with 2% urethane and mounted in a chamber that pressed them between a coverslip and mesh. Using this method, we were able to visualize living neurons in the context of the entire body of a juvenile polyp (Fig. 3B). Sparse spacing of labeled LWamide-like+ neurons in the body column of mosaic polyps facilitated identification and tracing of neurites from individual cells, so we limited our analysis to neurons in this region. NvEB1-GFP puncta, or comets, consistent with binding of NvEB1-GFP to microtubules were observed, and we performed live imaging of bipolar and tripolar neuron neurites in whole juvenile polyps at the 4–6 tentacle stage to determine microtubule polarity. Moving NvEB1-GFP comets were seen in labeled neurons (Fig. 3C), and their speed (Fig. 3D) was consistent with that of growing microtubule plus ends (Feng et al., 2019). The vast majority of NvEB1-GFP comets in LWamide-like+ ganglion neurons moved away from the cell body (blue arrowheads, Fig. 3C,E and Movie 1) consistent with a plus-end-out microtubule orientation. We examined all neurites of 13 bipolar and 13 tripolar LWamide-like+ ganglion neurons and found microtubule polarity to be close to 90% plus-end-out in all neurites in both cellular geometries (Fig. 3E). This percentage of plus-end-out microtubules is similar to that observed for bilaterian axons and distinctly different from bilaterian dendrites. In *Drosophila*, *C. elegans* and vertebrate axons, >95% of microtubules are plus-end out (Baas and Lin, 2011; Harterink et al., 2018; Stone et al., 2008) whereas microtubules in dendrites range from evenly mixed polarity in mammals (Baas and Lin, 2011; Yau et al., 2016) to almost completely minus-end out in *Drosophila* and *C. elegans* (Goodwin et al., 2012; Harterink et al., 2018; Rolls et al., 2007; Stone et al., 2008).

In many of the bipolar and tripolar cells, NvEB1-GFP comets were observed radiating from a point in the cell body, consistent with a single MTOC. This MTOC is likely the centrosome, although

Journal of Experimental Biology (2020) 223, jeb233197. doi:10.1242/jeb.233197

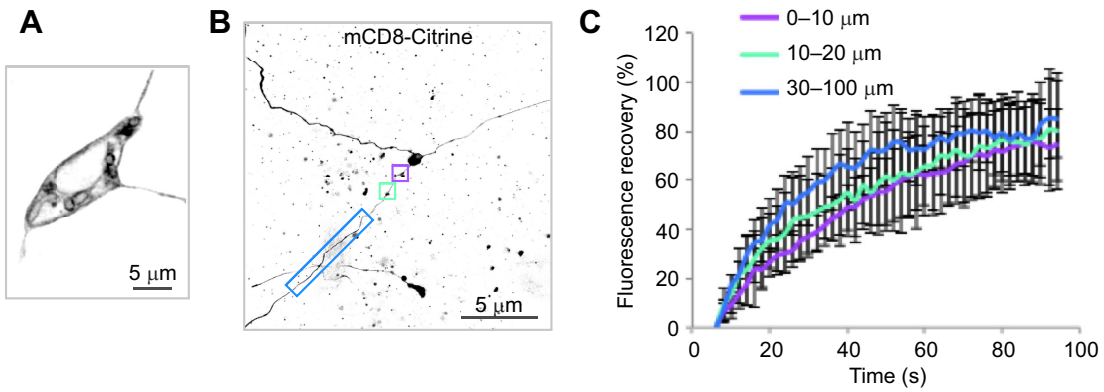

Fig. 4. Plus-end-out neurites of tripolar LWamide-like+ ganglion neurons lack a diffusion barrier. (A) mCD8-Citrine localizes to the plasma membrane of tripolar LWamide-like+ neurons expressing NvLWamide-like::mCD8-citrine. It is concentrated at the cell periphery and can also be seen in internal membranes, likely including the endoplasmic reticulum and Golgi where it is synthesized and processed. (B) FRAP was performed by bleaching 5 µm segments of all three neurites in regions 0–10 µm (purple box), 10–20 µm (turquoise box) and 30–100 µm (blue box) from the cell body. (C) Quantification of mCD8-Citrine fluorescence recovery after photobleaching. Results were normalized by setting fluorescence intensity after bleaching to 0. Average recovery is shown, with error bars representing s.d. (*N*=6 cells for 0–10 µm and 10–30 µm, *N*=4 for 30–100 µm; FRAP was performed in all neurites of each cell).

the Golgi or another organelle cannot be ruled out. In mammals, centrosomes are gradually inactivated as MTOCs during neuronal maturation (Stiess et al., 2010). This inactivation likely occurs as nucleation sites associate with other cellular structures, perhaps endosomes, which house nucleation sites in *Drosophila* and *C. elegans* dendrites (Liang et al., 2020; Weiner et al., 2020). To determine whether the somatic MTOC remained active over time, we imaged the cell body of three bipolar cells and two tripolar cells at two time points, day 0 and again at day 5 (Fig. 3F and Movie 2). Cells were identified based on position in the body relative to a clipped tentacle. In all cases the MTOC was still present at day 5. Maintenance of a single somatic MTOC over time distinguishes these neurons from those in bilaterians examined to date. The somatic MTOC may contribute to the maintenance of the plus-end-out microtubule array in LWamide-like+ ganglion neurons.

Plus-end-out neurites of tripolar ganglion neurons lack a diffusion barrier

Because the microtubules have an axon-like plus-end-out arrangement in the neurites of LWamide-like+ neurons, we next examined whether neurites in these cells have a plasma membrane diffusion barrier. In both vertebrate and bilaterian invertebrate neurons, a diffusion barrier has been shown to exist in the plasma membrane of the proximal axon (axon initial segment, AIS) to separate the somatodendritic and axonal plasma membranes (Jegla et al., 2016; Winckler et al., 1999). In bilaterians, this diffusion barrier is organized primarily by the giant ankyrin-based cytoskeleton (Jegla et al., 2016; Song et al., 2009). Cnidarian genomes contain an ankyrin gene, but it is not predicted to encode a giant isoform (Jegla et al., 2016). However, this does not exclude the possible formation of a diffusion barrier or proto-AIS being organized by shorter isoforms of ankyrin.

We tested for the presence of a diffusion barrier in tripolar cells using FRAP. mCD8-Citrine localizes to the plasma membrane of LWamide-like+ tripolar neurons (Fig. 4A). FRAP of tagged mCD8 was previously used to identify a diffusion barrier in developing *Drosophila* axons (Katsuki et al., 2009) and at the base of mature *Drosophila* axons (Jegla et al., 2016). The diffusion barriers were detected based on very limited recovery (<30%) of fluorescence in the region over a period of several minutes. We performed FRAP experiments in live juvenile polyps by bleaching 5 µm segments of all three neurites in regions 0–10 µm (6 neurons), 10–20 µm (6 neurons) or 30–100 µm (4 neurons) from the cell body (Fig. 4B) and measured recovery of mCD8-Citrine fluorescence. At all regions along the three neurites, fluorescence recovered >70% by 90 s (Fig. 4C), indicating that plasma membrane diffusion barriers are not present in any of the neurites extending from these neurons. Thus, it appears that LWamide-like+ neurons extend neurites with uniform axon-like microtubule polarity (Fig. 3), but without bilaterian-like axonal plasma membrane diffusion barriers to separate the neurite membrane from the soma (Fig. 4).

Presynaptic and postsynaptic markers localize to varicosities in all three neurites of tripolar ganglion neurons

In most bilaterian neurons, synaptic components are partitioned to distinct compartments: presynaptic proteins localize to the axon while postsynaptic components localize to dendrites. However, owing to the equivalent microtubule arrangement and absence of diffusion barrier in neurites of LWamide-like+ tripolar ganglion neurons, we hypothesized that presynaptic and postsynaptic proteins would be found equally among all three neurites. We looked for presynaptic sites in LWamide-like+ tripolar ganglion neurons using NvLWamide-like::NvSynaptobrevin-mCherry. We looked at seven tripolar neurons and red puncta were present in all three neurites of each neuron (Fig. 5A) and often localized to varicosities along the neurites (Fig. 5A, arrowheads). In two cells, NvSynaptobrevin-mCherry was observed at varicosities where neurites crossed (Fig. 5B, Movie 3) and we hypothesize that these could represent en passant synapses similar to those described in the jellyfish Cyanea, where bidirectional chemical synapses form in the motor nerve net wherever neurites touch (Anderson, 1985; Anderson and Spencer, 1989). Occasionally, vesicles were observed being transported along neurites. However, the majority of moving vesicles were observed in the cell body or at varicosities in the neurites (Fig. 5, Movie 3) of the tripolar neurons we imaged, consistent with varicosities being synapses. An NvLWamide-like-Emerald fusion protein designed to load into presynaptic vesicles showed a similar expression pattern in LWamide-like+ tripolar neurons to NvSynaptobrevin-mCherry: it was observed in all three neurites of nine tripolar neurons (Fig. 5C) and frequently localized to varicosities (Fig. 5C inset and Movie 4). Again, moving vesicles were observed at these varicosities (Movie 4) similar to

Journal of Experimental Biology (2020) 223, jeb233197. doi:10.1242/jeb.233197

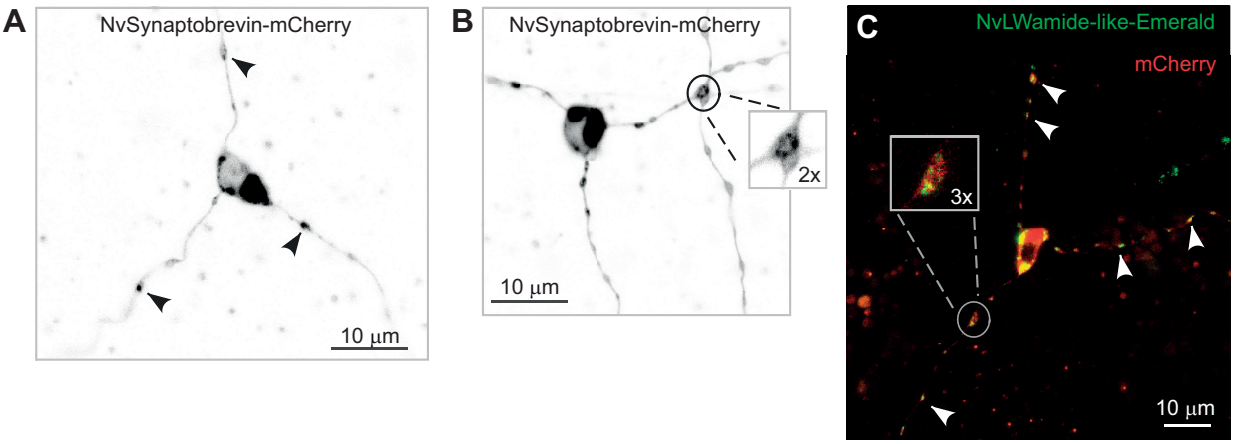

Fig. 5. Presynaptic markers localize to all three neurites of tripolar LWamide-like+ ganglion neurons. (A) Tripolar ganglion neuron expressing NvLWamide-like::NvSynaptobrevin-mCherry. NvSynaptobrevin-mCherry is present in all three neurites and can be seen at varicosities along the neurites indicated by black arrowheads. (B) NvSynaptobrevin-mCherry can also be seen at varicosities where two neurites cross (inset). (C) Tripolar ganglion neuron expressing NvLWamide-like::NvLWamide-like-Emerald and cytoplasmic mCherry. NvLWamide-like-Emerald GFP localizes to all three neurites (white arrowheads) and is often seen at varicosities along the neurites (inset). mCherry distribution is broader and visible wherever significant cytoplasmic volume was present.

NvSynaptobrevin-mCherry where moving vesicles were most often seen in the cell body and at varicosities. In addition, NvLWamide-like::NvLWamide-like-Emerald was also observed in both neurites of three bipolar neurons.

The candidate postsynaptic marker NvHomer-GFP was distributed to all three neurites in two of five tripolar neurons imaged (Fig. 6A). Of the remaining three neurons, two had NvHomer-GFP in two neurites and one in a single neurite. We also identified four bipolar neurons with NvHomer-GFP in both neurites. Within neurites that contained NvHomer-GFP, only a subset of varicosities contained the marker. This is in contrast to NvLWamide-like-Emerald, which was typically found in all varicosities along a neurite. It is likely that localization of NvHomer-GFP is more sensitive to expression level than the neuropeptide, and GFP-tagging could also affect robustness of NvHomer targeting. However, we did identify NvHomer-GFP puncta at varicosities where neurites cross (Fig. 6B) suggesting that varicosities containing NvHomer-GFP are likely to be synapses.

In order to test the hypothesis that NvSynaptobrevin, LWamide-like-Emerald and NvHomer-GFP co-localize to synaptic sites in LWamide-like+ neurons, we used a single plasmid to drive mosaic expression of NvLWamide-like::NvHomer-GFP and NvElav1::NvSynaptobrevin-mCherry. The Elav1 promoter is widely expressed in the *Nematostella* nervous system (Nakanishi et al., 2012). Following injection with the double expression construct, we observed independently varying levels of expression of the two transgenes in neurons. We observed a large proportion of neurons that expressed either NvSynaptobrevin-mCherry or NvHomer-GFP alone (Fig. 6C), and a smaller subset of neurons that expressed both markers (Fig. 6D). In neurons expressing both markers, we found four examples where NvSynaptobrevin-mCherry and NvHomer-GFP co-localized to varicosities along the neurites, suggesting that these varicosities contain both presynaptic and postsynaptic components as might be expected at bidirectional synapses (Fig. 6D). Finally, we were able to visualize four examples of neurites crossing where both NvSynaptobrevin-mCherry and NvHomer-GFP were present. In two examples of crossing neurites, each cell expressed only one of the markers (Fig. 6E) meaning that the two markers localized at separate sides of a contact site from each other. In the other two examples, each cell expressed both markers and they co-localized to the crossing. In both of these scenarios, the presence of NvSynaptobrevin-mCherry and NvHomer-GFP at the crossing contacts between the neurites (Fig. 6E) suggests that these crossing sites are indeed chemical synapses.

DISCUSSION

We have developed tools to determine whether LWamide-like+ bipolar and tripolar ganglion neurons in the cnidarian *Nematostella vectensis* share key features of axo-dendritic polarity found in bilaterian neurons. These features include different arrangements of microtubules in axons and dendrites, a diffusion barrier at the beginning of the axon, and differential distribution of pre- and postsynaptic machinery to axons and dendrites. Using these tools, we found that microtubules are oriented plus-end-out in all neurites (Fig. 3), similar to the axonal arrangement in bilaterians. However, unlike these axons, no diffusion barrier was detected, and so it is likely that no large-scale specialization of the plasma membrane is present. As microtubules provide tracks for transport of cargoes such as proteins and organelles, identical microtubule orientation in all neurites suggests that they have the same contents. Indeed, when we looked at pre- and postsynaptic machinery (Figs 5 and 6), it was equally distributed among all neurites in many neurons.

While assaying microtubule polarity with NvEB1-GFP, we observed a single MTOC in the cell body of tripolar ganglion neurons (Fig. 3). The most likely identity of this MTOC is the centrosome. Microtubules originating at the centrosome would grow into neurites in a plus-end-out orientation, and this could help establish and maintain polarity. The centrosome is the major site of nucleation and source of axonal microtubules in developing mammalian neurons (Ahmad and Baas, 1995; Ahmad et al., 1994). However, as these neurons mature, the centrosome is inactivated as a nucleation site (Stiess et al., 2010). In bilaterian invertebrates like *Drosophila*, it is unclear whether the centrosome plays any role in neurons (Basto et al., 2006; Nguyen et al., 2011). Therefore, it is interesting to find an MTOC in the cell body of the tripolar LWamide-like+ ganglion neurons in *Nematostella* that remains active over the course of 5 days. One hypothesis is that maintenance of the MTOC helps organize the plus-end-out microtubule array in the neurites by contributing new plus ends to each of the processes. However, because the neurites extend long distances over the body of the animal, it is likely that other

Journal of Experimental Biology (2020) 223, jeb233197. doi:10.1242/jeb.233197

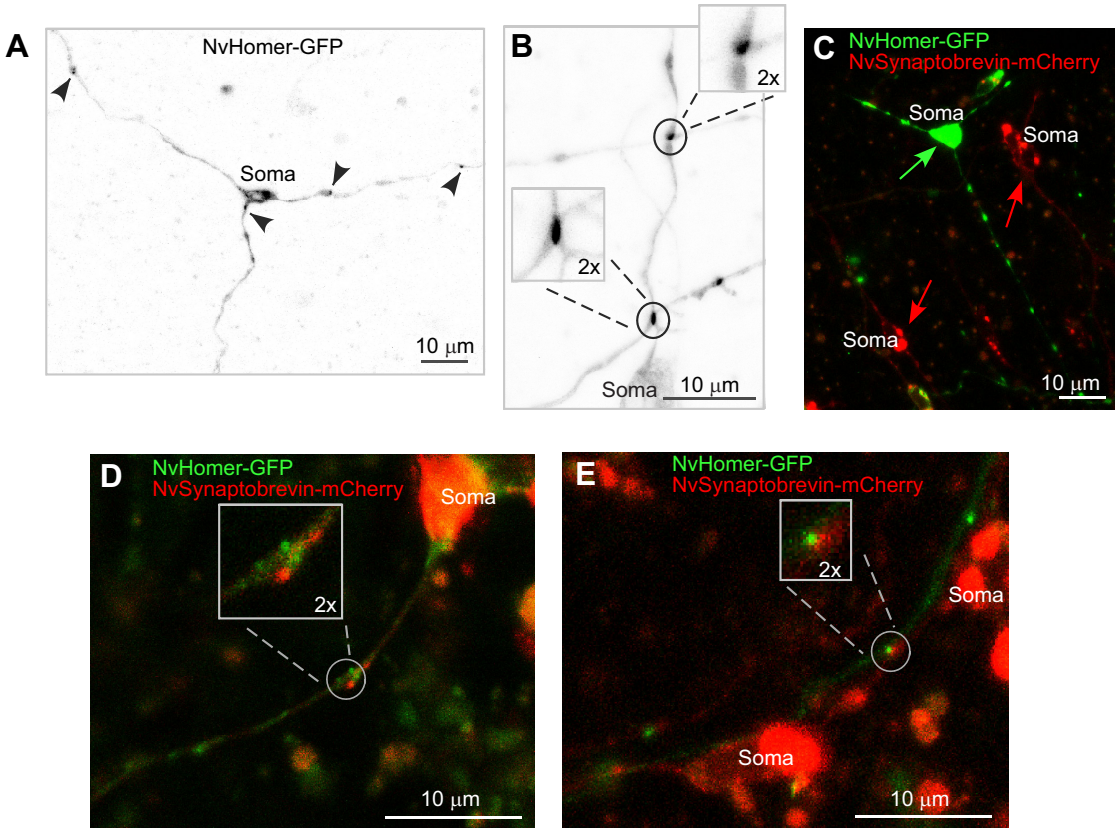

Fig. 6. Postsynaptic marker NvHomer-GFP localizes to all three neurites of tripolar LWamide-like+ ganglion neurons. (A) Tripolar ganglion neuron expressing NvLWamide-like::NvHomer-GFP. NvHomer-GFP localizes to all three neurites as indicated by black arrowheads. (B) NvHomer-GFP puncta can be seen at sites of neurites crossing (insets). (C) Injection of a double expression construct for NvLWamide-like::NvHomer-GFP and NvElav1::NvSynaptobrevin-mCherry yields varying levels of expression. Here, a representative mosaic polyp is shown where the green arrow indicates a tripolar ganglion neuron expressing only NvLWamide-like::NvHomer-GFP and red arrows indicate neurons expressing only NvElav1::NvSynaptobrevin-mCherry. (D) Example of bipolar ganglion neuron expressing both NvLWamide-like::NvHomer-GFP and NvElav1::NvSynaptobrevin-mCherry. Inset shows both markers localizing to the same varicosity along a neurite. (E) NvHomer-GFP and NvSynaptobrevin-mCherry are both present at a neurite crossing (inset). In this example, a neuron expressing only NvLWamide-like::NvHomer-GFP can be seen crossing a neuron expressing only NvElav1::NvSynaptobrevin-mCherry.

mechanisms regulate microtubule polarity further from the cell body. Augmin-mediated nucleation from the sides of existing microtubules plays a role in regulation of the plus-end-out microtubule array in axons of cultured mouse hippocampal neurons (Sanchez-Huertas et al., 2016) and augmin-mediated nucleation would be expected to reinforce existing polarity (Petry et al., 2013) so could propagate plus-end-out polarity from the base of the axon outwards.

Although having all neurites with similar microtubule polarity distinguishes *Nematostella* LWamide-like+ ganglion neurons from most bilaterian neurons, at least one vertebrate neuron type also has all plus-end-out neurites. Rohon-Beard (RB) neurons are found in larval fish and amphibians and are transient pseudo-unipolar somatosensory neurons that have central axons projecting to the spinal cord and peripheral axons to the skin. Using EB3-GFP in RB neurons of zebrafish, it was shown that microtubules are oriented as plus-end-out in both non-branching central axons and branching peripheral axons (Lee et al., 2017). Despite this uniform microtubule polarity, the different processes are able to perform polarized functions, with the peripheral axons receiving sensory input from the skin and the central axons sending signals to the brain. This contrasts with LWamide-like+ ganglion neurons in *Nematostella*, which have three equal neurites with similar microtubule polarity, similar contents, similar lack of branching and likely also similar function.

Our results suggest the network of LWamide-like+ neurons within the nerve net of *Nematostella* is unpolarized at the cellular level and connected at least in part by bidirectional synapses. The functional significance of this network is not yet clear, because the activity of LWamide-like+ neurons has not yet been associated with specific polyp behaviors. Previous studies have described bidirectional synapses throughout the phylum Cnidaria, including scyphomedusae (Anderson, 1985; Anderson and Grünert, 1988; Horridge et al., 1962), hydromedusae (Jha and Mackie, 1967), cubomedusae (Satterlie, 1979) and hydroids (Kinnamon and Westfall, 1982; Westfall, 1973), but the behavioral role of bidirectional signaling in cnidarians is still poorly understood. In the Scyphozoan jellyfish Cyanea, the unpolarized swim motor neuron network appears to serve simply as a conduit between pacemaker neurons and muscle (Anderson, 1985; Anderson and Spencer, 1989). Bidirectional signaling between swim motor neurons may facilitate spread of neuronal activity throughout the network regardless of the site of origin to coordinate a swimming response. Bidirectional signaling has also been observed in parts of the hydra nerve net and may allow the point of origin of activity within a network to influence the behavioral sequence (Dupre and Yuste, 2017). We hypothesize that the LWamide-like+ ganglion neurons might act as an unpolarized network designed to facilitate conduction of signals across the body column regardless of the point of signal origin. While we show here that these ganglion neurons are

likely connected to each other via bidirectional synapses, a complete characterization of their synaptic connectivity, including identification of the inputs and outputs of the network, will be needed to develop refined hypotheses of the role of the network that can be tested through the effect of genetic manipulations on behavior.

While the LWamide-like+ neurons we have characterized are unpolarized with axon-like microtubule arrays, it is important to note that we have examined only a small fraction of the neuronal diversity in the nerve net; *Nematostella* has close to 30 other transcriptionally distinct neuronal types (Sebe-Pedros et al., 2018). It therefore remains to be determined if other neuronal cell types have more polarized cellular anatomy with segregation of presynaptic and postsynaptic sites. Polar chemical synapses have indeed been identified in some cnidarians (Anderson and Spencer, 1989). Perhaps sensory neurons or cnidocytes, cells that occupy terminal positions within the signaling network, will have polarized characteristics for directional signaling. It will also be interesting to see if all cnidarian neurons adopt an axon-like plus-end-out microtubule polarity, or if some neuronal types extend dendrite-like mixed polarity or minus-end-out neurites instead of or in addition to axon-like neurites. The presence of neurons with dendrite-like microtubule polarity in cnidarians would suggest the building blocks for bilaterian-style axodendritic polarity evolved prior to the cnidarian–bilaterian divergence in comparatively simple ancestral nerve nets. However, if cnidarian neurons are proven to only extend axon-like processes, then it would suggest that dendrites could be a bilaterian-specific innovation for polarized signaling.

Acknowledgements
We are grateful to Mark Martindale, University of Florida, for animals to start our sea anemone colony, and Michael Layden, Lehigh University, for providing us with the LWamide-like promoter region. We thank Benjamin Simonson for help with animal maintenance and Jose Chu Luo and Emma Baser for assistance with cloning.

Competing interests
The authors declare no competing or financial interests.

Author contributions
Conceptualization: M.M.R., T.J.; Formal analysis: M.C.S.; Investigation: M.C.S., G.O.K.; Writing - original draft: M.C.S.; Writing - review & editing: M.M.R., T.J.; Supervision: M.M.R., T.J.; Funding acquisition: M.M.R., T.J.

Funding
Funding was provided by the National Institute of General Medical Sciences (R01 GM085115 to M.M.R.) and by the National Institute of Neurological Disorders and Stroke (R21 NS093447 to M.M.R. and T.J.). Deposited in PMC for release after 12 months.

Supplementary information
Supplementary information available online at
https://jeb.biologists.org/lookup/doi/10.1242/jeb.233197.supplemental

References
Ahmad, F. J. and Baas, P. W. (1995). Microtubules released from the neuronal centrosome are transported into the axon. *J. Cell Sci.* **108**, 2761-2769.
Ahmad, F. J., Joshi, H. C., Centonze, V. E. and Baas, P. W. (1994). Inhibition of microtubule nucleation at the neuronal centrosome compromises axon growth. *Neuron* **12**, 271-280. doi:10.1016/0896-6273(94)90270-4
Anderson, P. A. (1985). Physiology of a bidirectional, excitatory, chemical synapse. *J. Neurophysiol.* **53**, 821-835. doi:10.1152/jn.1985.53.3.821
Anderson, P. A. V. and Grünert, U. (1988). Three-dimensional structure of bidirectional, excitatory chemical synapses in the jellyfish Cyanea capillata. *Synapse* **2**, 606-613. doi:10.1002/syn.890020605
Anderson, P. A. V. and Spencer, A. N. (1989). The importance of cnidarian synapses for neurobiology. *J. Neurobiol.* **20**, 435-457. doi:10.1002/neu.480200513
Baas, P. W. and Lin, S. (2011). Hooks and comets: the story of microtubule polarity orientation in the neuron. *Dev. Neurobiol.* **71**, 403-418. doi:10.1002/dneu.20818
Baas, P. W., Deitch, J. S., Black, M. M. and Banker, G. A. (1988). Polarity orientation of microtubules in hippocampal neurons: uniformity in the axon and nonuniformity in the dendrite. *Proc. Natl. Acad. Sci. USA* **85**, 8335-8339. doi:10.1073/pnas.85.21.8335
Baker, E. C., Layden, M. J., van Rossum, D. B., Kamel, B., Medina, M., Simpson, E. and Jegla, T. (2015). Functional characterization of cnidarian HCN channels points to an early evolution of Ih. *PLoS ONE* **10**, e0142730. doi:10.1371/journal.pone.0142730
Bartlett, W. P. and Banker, G. A. (1984). An electron microscopic study of the development of axons and dendrites by hippocampal neurons in culture. I. Cells which develop without intercellular contacts. *J. Neurosci.* **4**, 1944-1953. doi:10.1523/JNEUROSCI.04-08-01944.1984
Basto, R., Lau, J., Vinogradova, T., Gardiol, A., Woods, C. G., Khodjakov, A. and Raff, J. W. (2006). Flies without centrioles. *Cell* **125**, 1375-1386. doi:10.1016/j.cell.2006.05.025
Bender, K. J. and Trussell, L. O. (2012). The physiology of the axon initial segment. *Annu. Rev. Neurosci.* **35**, 249-265. doi:10.1146/annurev-neuro-062111-150339
Bennett, V. and Lorenzo, D. N. (2013). Spectrin- and ankyrin-based membrane domains and the evolution of vertebrates. *Curr. Top. Membr.* **72**, 1-37. doi:10.1016/B978-0-12-417027-8.00001-5
Berghs, S., Aggujaro, D., Dirkx, R., , Jr., Maksimova, E., Stabach, P., Hermel, J.-M., Zhang, J.-P., Philbrick, W., Slepnev, V., Ort, T. et al. (2000). βIV spectrin, a new spectrin localized at axon initial segments and nodes of ranvier in the central and peripheral nervous system. *J. Cell Biol.* **151**, 985-1002. doi:10.1083/jcb.151.5.985
Brakeman, P. R., Lanahan, A. A., O'Brien, R., Roche, K., Barnes, C. A., Huganir, R. L. and Worley, P. F. (1997). Homer: a protein that selectively binds metabotropic glutamate receptors. *Nature* **386**, 284-288. doi:10.1038/386284a0
Burkhardt, P., Grønborg, M., McDonald, K., Sulur, T., Wang, Q. and King, N. (2014). Evolutionary insights into premetazoan functions of the neuronal protein homer. *Mol. Biol. Evol.* **31**, 2342-2355. doi:10.1093/molbev/msu178
Burton, P. R. (1988). Dendrites of mitral cell neurons contain microtubules of opposite polarity. *Brain Res.* **473**, 107-115. doi:10.1016/0006-8993(88)90321-6
Cameron, P., Mundigl, O. and De Camilli, P. (1993). Traffic of synaptic vesicle proteins in polarized and nonpolarized cells. *J. Cell Sci.* **17**, 93-100. doi:10.1242/jcs.1993.Supplement_17.14
Chapman, J. A., Kirkness, E. F., Simakov, O., Hampson, S. E., Mitros, T., Weinmaier, T., Rattei, T., Balasubramanian, P. G., Borman, J., Busam, D. et al. (2010). The dynamic genome of Hydra. *Nature* **464**, 592-596. doi:10.1038/nature08830
Cole, A. G., Kaul, S., Jahnel, S. M., Steger, J., Zimmerman, B., Reischl, R., Richards, G. S., Rentzsch, F., Steinmetz, P. and Technau, U. (2020). Muscle cell type diversification facilitated by extensive gene duplications. *bioRxiv* 2020.07.19.210658. doi:10.1101/2020.07.19.210658
Craig, A. M. and Banker, G. (1994). Neuronal polarity. *Annu. Rev. Neurosci.* **17**, 267-310. doi:10.1146/annurev.ne.17.030194.001411
Daniels, R. W., Rossano, A. J., Macleod, G. T. and Ganetzky, B. (2014). Expression of multiple transgenes from a single construct using viral 2A peptides in Drosophila. *PLoS ONE* **9**, e100637. doi:10.1371/journal.pone.0100637
Diagana, T. T., Thomas, U., Prokopenko, S. N., Xiao, B., Worley, P. F. and Thomas, J. B. (2002). Mutation of Drosophila homer disrupts control of locomotor activity and behavioral plasticity. *J. Neurosci.* **22**, 428-436. doi:10.1523/JNEUROSCI.22-02-00428.2002
Dodson, P. D., Barker, M. C. and Forsythe, I. D. (2002). Two heteromeric Kv1 potassium channels differentially regulate action potential firing. *J. Neurosci.* **22**, 6953-6961. doi:10.1523/JNEUROSCI.22-16-06953.2002
DuBuc, T. Q., Dattoli, A. A., Babonis, L. S., Salinas-Saavedra, M., Röttinger, E., Martindale, M. Q. and Postma, M. (2014). In vivo imaging of Nematostella vectensis embryogenesis and late development using fluorescent probes. *BMC Cell Biol.* **15**, 44. doi:10.1186/s12860-014-0044-2
Dupre, C. and Yuste, R. (2017). Non-overlapping Neural Networks in Hydra vulgaris. *Curr. Biol.* **27**, 1085-1097. doi:10.1016/j.cub.2017.02.049
Estes, P. S., Ho, G. L. Y., Narayanan, R. and Ramaswami, M. (2000). Synaptic localization and restricted diffusion of a Drosophila neuronal synaptobrevin–green fluorescent protein chimera in vivo. *J. Neurogenet.* **13**, 233-255. doi:10.3109/01677060009084496
Feng, C., Thyagarajan, P., Shorey, M., Seebold, D. Y., Weiner, A. T., Albertson, R. M., Rao, K. S., Sagasti, A., Goetschius, D. J. and Rolls, M. M. (2019). Patronin-mediated minus end growth is required for dendritic microtubule polarity. *J. Cell Biol.* **218**, 2309-2328. doi:10.1083/jcb.201810155
Fritzenwanker, J. H. and Technau, U. (2002). Induction of gametogenesis in the basal cnidarian Nematostella vectensis (Anthozoa). *Dev. Genes Evol.* **212**, 99-103. doi:10.1007/s00427-002-0214-7
Gajewski, M., Leitz, T., Schloßherr, J. and Plickert, G. (1996). LWamides from Cnidaria constitute a novel family of neuropeptides with morphogenetic activity. *Roux Arch. Dev. Biol.* **205**, 232-242. doi:10.1007/BF00365801
Galjart, N. (2010). Plus-end-tracking proteins and their interactions at microtubule ends. *Curr. Biol.* **20**, R528-R537. doi:10.1016/j.cub.2010.05.022
Goldberg, E. M., Clark, B. D., Zagha, E., Nahmani, M., Erisir, A. and Rudy, B. (2008). K+ channels at the axon initial segment dampen near-threshold

excitability of neocortical fast-spiking GABAergic interneurons. *Neuron* **58**, 387-400. doi:10.1016/j.neuron.2008.03.003

Goodwin, P. R., Sasaki, J. M. and Juo, P. (2012). Cyclin-dependent kinase 5 regulates the polarized trafficking of neuropeptide-containing dense-core vesicles in Caenorhabditis elegans motor neurons. *J. Neurosci.* **32**, 8158-8172. doi:10.1523/JNEUROSCI.0251-12.2012

Griesbeck, O., Baird, G. S., Campbell, R. E., Zacharias, D. A. and Tsien, R. Y. (2001). Reducing the environmental sensitivity of yellow fluorescent protein. Mechanism and applications. *J. Biol. Chem.* **276**, 29188-29194. doi:10.1074/jbc.M102815200

Grubb, M. S. and Burrone, J. (2010). Building and maintaining the axon initial segment. *Curr. Opin. Neurobiol.* **20**, 481-488. doi:10.1016/j.conb.2010.04.012

Gur Barzilai, M., Reitzel, A. M., Kraus, J. E. M., Gordon, D., Technau, U., Gurevitz, M. and Moran, Y. (2012). Convergent evolution of sodium ion selectivity in metazoan neuronal signaling. *Cell Rep.* **2**, 242-248. doi:10.1016/j.celrep.2012.06.016

Han, W., Ng, Y.-K., Axelrod, D. and Levitan, E. S. (1999). Neuropeptide release by efficient recruitment of diffusing cytoplasmic secretory vesicles. *Proc. Natl. Acad. Sci. USA* **96**, 14577-14582. doi:10.1073/pnas.96.25.14577

Hand, C. and Uhlinger, K. R. (1992). The culture, sexual and asexual reproduction, and growth of the sea anemone nematostella vectensis. *Biol. Bull.* **182**, 169-176. doi:10.2307/1542110

Harterink, M., Edwards, S. L., de Haan, B., Yau, K. W., van den Heuvel, S., Kapitein, L. C., Miller, K. G. and Hoogenraad, C. C. (2018). Local microtubule organization promotes cargo transport in C. elegans dendrites. *J. Cell Sci.* **131**, jcs223107. doi:10.1242/jcs.223107

Havrilak, J. A., Faltine-Gonzalez, D., Wen, Y., Fodera, D., Simpson, A. C., Magie, C. R. and Layden, M. J. (2017). Characterization of NvLWamide-like neurons reveals stereotypy in Nematostella nerve net development. *Dev. Biol.* **431**, 336-346. doi:10.1016/j.ydbio.2017.08.028

Hayashi, M. K., Tang, C., Verpelli, C., Narayanan, R., Stearns, M. H., Xu, R.-M., Li, H., Sala, C. and Hayashi, Y. (2009). The postsynaptic density proteins Homer and Shank form a polymeric network structure. *Cell* **137**, 159-171. doi:10.1016/j.cell.2009.01.050

Horridge, G. A., Chapman, D. M. and Mackay, B. (1962). Naked axons and symmetrical synapses in an elementary nervous system. *Nature* **193**, 899-900. doi:10.1038/193899a0

Inan, M., Blazquez-Llorca, L., Merchan-Perez, A., Anderson, S. A., DeFelipe, J. and Yuste, R. (2013). Dense and overlapping innervation of pyramidal neurons by chandelier cells. *J. Neurosci.* **33**, 1907-1914. doi:10.1523/JNEUROSCI.4049-12.2013

Jegla, T. and Salkoff, L. (1997). A novel subunit for shal K+ channels radically alters activation and inactivation. *J. Neurosci.* **17**, 32-44. doi:10.1523/JNEUROSCI.17-01-00032.1997

Jegla, T., Grigoriev, N., Gallin, W. J., Salkoff, L. and Spencer, A. N. (1995). Multiple Shaker potassium channels in a primitive metazoan. *J. Neurosci.* **15**, 7989-7999. doi:10.1523/JNEUROSCI.15-12-07989.1995

Jegla, T. J., Zmasek, C. M., Batalov, S. and Nayak, S. K. (2009). Evolution of the human ion channel set. *Comb. Chem. High Throughput Screen.* **12**, 2-23. doi:10.2174/138620709787047957

Jegla, T., Marlow, H. Q., Chen, B., Simmons, D. K., Jacobo, S. M. and Martindale, M. Q. (2012). Expanded functional diversity of shaker K+ channels in cnidarians is driven by gene expansion. *PLoS ONE* **7**, e51366. doi:10.1371/journal.pone.0051366

Jegla, T., Nguyen, M. M., Feng, C., Goetschius, D. J., Luna, E., van Rossum, D. B., Kamel, B., Pisupati, A., Milner, E. S. and Rolls, M. M. (2016). Bilaterian giant ankyrins have a common evolutionary origin and play a conserved role in patterning the axon initial segment. *PLoS Genet.* **12**, e1006457. doi:10.1371/journal.pgen.1006457

Jenkins, P. M., Kim, N., Jones, S. L., Tseng, W. C., Svitkina, T. M., Yin, H. H. and Bennett, V. (2015). Giant ankyrin-G: a critical innovation in vertebrate evolution of fast and integrated neuronal signaling. *Proc. Natl. Acad. Sci. USA* **112**, 957-964. doi:10.1073/pnas.1416544112

Jha, R. K. and Mackie, G. O. (1967). The recognition, distribution and ultrastructure of hydrozoan nerve elements. *J. Morphol.* **123**, 43-61. doi:10.1002/jmor.1051230105

Jiang, K. and Akhmanova, A. (2011). Microtubule tip-interacting proteins: a view from both ends. *Curr. Opin. Cell Biol.* **23**, 94-101. doi:10.1016/j.ceb.2010.08.008

Johnston, J., Griffin, S. J., Baker, C., Skrzypiec, A., Chernova, T. and Forsythe, I. D. (2008). Initial segment Kv2.2 channels mediate a slow delayed rectifier and maintain high frequency action potential firing in medial nucleus of the trapezoid body neurons. *J. Physiol.* **586**, 3493-3509. doi:10.1113/jphysiol.2008.153734

Kapitein, L. C., Schlager, M. A., Kuijpers, M., Wulf, P. S., van Spronsen, M., MacKintosh, F. C. and Hoogenraad, C. C. (2010). Mixed microtubules steer dynein-driven cargo transport into dendrites. *Curr. Biol.* **20**, 290-299. doi:10.1016/j.cub.2009.12.052

Katsuki, T., Ailani, D., Hiramoto, M. and Hiromi, Y. (2009). Intra-axonal patterning: intrinsic compartmentalization of the axonal membrane in Drosophila neurons. *Neuron* **64**, 188-199. doi:10.1016/j.neuron.2009.08.019

Kelava, I., Rentzsch, F. and Technau, U. (2015). Evolution of eumetazoan nervous systems: insights from cnidarians. *Philos. Trans. R. Soc. Lond. B Biol. Sci.* **370**, 20150065. doi:10.1098/rstb.2015.0065

Kinnamon, J. C. and Westfall, J. A. (1982). Types of neurons and synaptic connections at hypostome-tentacle junctions in Hydra. *J. Morphol.* **173**, 119-128. doi:10.1002/jmor.1051730110

Kobayashi, T., Storrie, B., Simons, K. and Dotti, C. G. (1992). A functional barrier to movement of lipids in polarized neurons. *Nature* **359**, 647-650. doi:10.1038/359647a0

Kordeli, E., Lambert, S. and Bennett, V. (1995). AnkyrinG. A new ankyrin gene with neural-specific isoforms localized at the axonal initial segment and node of Ranvier. *J. Biol. Chem.* **270**, 2352-2359. doi:10.1074/jbc.270.5.2352

Layden, M. J. and Martindale, M. Q. (2014). Non-canonical Notch signaling represents an ancestral mechanism to regulate neural differentiation. *EvoDevo* **5**, 30. doi:10.1186/2041-9139-5-30

Layden, M. J., Boekhout, M. and Martindale, M. Q. (2012). Nematostella vectensis achaete-scute homolog NvashA regulates embryonic ectodermal neurogenesis and represents an ancient component of the metazoan neural specification pathway. *Development* **139**, 1013-1022. doi:10.1242/dev.073221

Layden, M. J., Röttinger, E., Wolenski, F. S., Gilmore, T. D. and Martindale, M. Q. (2013). Microinjection of mRNA or morpholinos for reverse genetic analysis in the starlet sea anemone, Nematostella vectensis. *Nat. Protoc.* **8**, 924-934. doi:10.1038/nprot.2013.009

Layden, M. J., Johnston, H., Amiel, A. R., Havrilak, J., Steinworth, B., Chock, T., Rottinger, E. and Martindale, M. Q. (2016a). MAPK signaling is necessary for neurogenesis in Nematostella vectensis. *BMC Biol.* **14**, 61. doi:10.1186/s12915-016-0282-1

Layden, M. J., Rentzsch, F. and Röttinger, E. (2016b). The rise of the starlet sea anemone Nematostella vectensis as a model system to investigate development and regeneration. *Wiley Interdiscip. Rev. Dev. Biol.* **5**, 408-428. doi:10.1002/wdev.222

Lee, T. and Luo, L. (1999). Mosaic analysis with a repressible cell marker for studies of gene function in neuronal morphogenesis. *Neuron* **22**, 451-461. doi:10.1016/S0896-6273(00)80701-1

Lee, T. J., Lee, J. W., Haynes, E. M., Eliceiri, K. W. and Halloran, M. C. (2017). The kinesin adaptor Calsyntenin-1 organizes microtubule polarity and regulates dynamics during sensory axon arbor development. *Front. Cell Neurosci.* **11**, 107. doi:10.3389/fncel.2017.00107

Leterrier, C. and Dargent, B. (2014). No Pasaran! Role of the axon initial segment in the regulation of protein transport and the maintenance of axonal identity. *Semin. Cell Dev. Biol.* **27**, 44-51. doi:10.1016/j.semcdb.2013.11.001

Li, X., Liu, H., Chu Luo, J., Rhodes, S. A., Trigg, L. M., van Rossum, D. B., Anishkin, A., Diatta, F. H., Sassic, J. K., Simmons, D. K. et al. (2015a). Major diversification of voltage-gated K+ channels occurred in ancestral parahoxozoans. *Proc. Natl. Acad. Sci. USA* **112**, E1010-E1019. doi:10.1073/pnas.1422941112

Li, X., Martinson, A. S., Layden, M. J., Diatta, F. H., Sberna, A. P., Simmons, D. K., Martindale, M. Q. and Jegla, T. J. (2015b). Ether-a-go-go family voltage-gated K+ channels evolved in an ancestral metazoan and functionally diversified in a cnidarian-bilaterian ancestor. *J. Exp. Biol.* **218**, 526-536. doi:10.1242/jeb.110080

Liang, X., Kokes, M., Fetter, R. D., Sallee, M. D., Moore, A. W., Feldman, J. L. and Shen, K. (2020). Growth cone-localized microtubule organizing center establishes microtubule orientation in dendrites. *Elife* **9**, e56547. doi:10.7554/eLife.56547.sa2

Liebeskind, B. J., Hillis, D. M. and Zakon, H. H. (2015). Convergence of ion channel genome content in early animal evolution. *Proc. Natl. Acad. Sci. USA* **112**, E846-E851. doi:10.1073/pnas.1501195112

Lin, S., Liu, M., Mozgova, O. I., Yu, W. and Baas, P. W. (2012). Mitotic motors coregulate microtubule patterns in axons and dendrites. *J. Neurosci.* **32**, 14033-14049. doi:10.1523/JNEUROSCI.3070-12.2012

Lorincz, A. and Nusser, Z. (2008). Cell-type-dependent molecular composition of the axon initial segment. *J. Neurosci.* **28**, 14329-14340. doi:10.1523/JNEUROSCI.4833-08.2008

Mackie, G. O. (2004). Central neural circuitry in the jellyfish Aglantha: a model 'simple nervous system'. *NeuroSignals* **13**, 5-19. doi:10.1159/000076155

Marlow, H. Q., Srivastava, M., Matus, D. Q., Rokhsar, D. and Martindale, M. Q. (2009). Anatomy and development of the nervous system of Nematostella vectensis, an anthozoan cnidarian. *Dev. Neurobiol.* **69**, 235-254. doi:10.1002/dneu.20698

Martinson, A. S., van Rossum, D. B., Diatta, F. H., Layden, M. J., Rhodes, S. A., Martindale, M. Q. and Jegla, T. (2014). Functional evolution of Erg potassium channel gating reveals an ancient origin for IKr. *Proc. Natl. Acad. Sci. USA* **111**, 5712-5717. doi:10.1073/pnas.1321716111

Mitgutsch, C., Hauser, F. and Grimmelikhuijzen, C. J. (1999). Expression and developmental regulation of the Hydra-RFamide and Hydra-LWamide preprohormone genes in Hydra: evidence for transient phases of head formation. *Dev. Biol.* **207**, 189-203. doi:10.1006/dbio.1998.9150

Moran, Y. and Zakon, H. H. (2014). The evolution of the four subunits of voltage-gated calcium channels: ancient roots, increasing complexity, and multiple losses. *Genome Biol. Evol.* **6**, 2210-2217. doi:10.1093/gbe/evu177
Moran, Y., Barzilai, M. G., Liebeskind, B. J. and Zakon, H. H. (2015). Evolution of voltage-gated ion channels at the emergence of Metazoa. *J. Exp. Biol.* **218**, 515-525. doi:10.1242/jeb.110270
Nakanishi, N., Renfer, E., Technau, U. and Rentzsch, F. (2012). Nervous systems of the sea anemone Nematostella vectensis are generated by ectoderm and endoderm and shaped by distinct mechanisms. *Development* **139**, 347-357. doi:10.1242/dev.071902
Nguyen, M. M., Stone, M. C. and Rolls, M. M. (2011). Microtubules are organized independently of the centrosome in Drosophila neurons. *Neural Dev.* **6**, 38. doi:10.1186/1749-8104-6-38
Nielsen, S. K. D., Koch, T. L., Hauser, F., Garm, A. and Grimmelikhuijzen, C. J. P. (2019). De novo transcriptome assembly of the cubomedusa Tripedalia cystophora, including the analysis of a set of genes involved in peptidergic neurotransmission. *BMC Genomics* **20**, 175. doi:10.1186/s12864-019-5514-7
Nonet, M. L. (1999). Visualization of synaptic specializations in live C. elegans with synaptic vesicle protein-GFP fusions. *J. Neurosci. Methods* **89**, 33-40. doi:10.1016/S0165-0270(99)00031-X
Norekian, T. P. and Moroz, L. L. (2020). Atlas of the neuromuscular system in the Trachymedusa Aglantha digitale: Insights from the advanced hydrozoan. *J. Comp. Neurol.* **528**, 1231-1254. doi:10.1002/cne.24821
Pan, Z., Kao, T., Horvath, Z., Lemos, J., Sul, J. Y., Cranstoun, S. D., Bennett, V., Scherer, S. S. and Cooper, E. C. (2006). A common ankyrin-G-based mechanism retains KCNQ and NaV channels at electrically active domains of the axon. *J. Neurosci.* **26**, 2599-2613. doi:10.1523/JNEUROSCI.4314-05.2006
Petry, S., Groen, A. C., Ishihara, K., Mitchison, T. J. and Vale, R. D. (2013). Branching microtubule nucleation in Xenopus egg extracts mediated by augmin and TPX2. *Cell* **152**, 768-777. doi:10.1016/j.cell.2012.12.044
Plickert, G., Schetter, E., Verhey-Van-Wijk, N., Schlossherr, J., Steinbüchel, M. and Gajewski, M. (2003). The role of alpha-amidated neuropeptides in hydroid development–LWamides and metamorphosis in Hydractinia echinata. *Int. J. Dev. Biol.* **47**, 439-450.
Putnam, N. H., Srivastava, M., Hellsten, U., Dirks, B., Chapman, J., Salamov, A., Terry, A., Shapiro, H., Lindquist, E., Kapitonov, V. V. et al. (2007). Sea anemone genome reveals ancestral eumetazoan gene repertoire and genomic organization. *Science* **317**, 86-94. doi:10.1126/science.1139158
Rao, S., Lang, C., Levitan, E. S. and Deitcher, D. L. (2001). Visualization of neuropeptide expression, transport, and exocytosis in Drosophila melanogaster. *J. Neurobiol.* **49**, 159-172. doi:10.1002/neu.1072
Rasband, M. N., Trimmer, J. S., Schwarz, T. L., Levinson, S. R., Ellisman, M. H., Schachner, M. and Shrager, P. (1998). Potassium channel distribution, clustering, and function in remyelinating rat axons. *J. Neurosci.* **18**, 36-47. doi:10.1523/JNEUROSCI.18-01-00036.1998
Ren, M., Yoshimura, Y., Takada, N., Horibe, S. and Komatsu, Y. (2007). Specialized inhibitory synaptic actions between nearby neocortical pyramidal neurons. *Science* **316**, 758-761. doi:10.1126/science.1135468
Renfer, E., Amon-Hassenzahl, A., Steinmetz, P. R. and Technau, U. (2010). A muscle-specific transgenic reporter line of the sea anemone, Nematostella vectensis. *Proc. Natl. Acad. Sci. USA* **107**, 104-108. doi:10.1073/pnas.0909148107
Rentzsch, F., Juliano, C. and Galliot, B. (2019). Modern genomic tools reveal the structural and cellular diversity of cnidarian nervous systems. *Curr. Opin. Neurobiol.* **56**, 87-96. doi:10.1016/j.conb.2018.12.004
Rolls, M. M. (2011). Neuronal polarity in Drosophila: sorting out axons and dendrites. *Dev. Neurobiol.* **71**, 419-429. doi:10.1002/dneu.20836
Rolls, M. M. and Jegla, T. J. (2015). Neuronal polarity: an evolutionary perspective. *J. Exp. Biol.* **218**, 572-580. doi:10.1242/jeb.112359
Rolls, M. M., Satoh, D., Clyne, P. J., Henner, A. L., Uemura, T. and Doe, C. Q. (2007). Polarity and intracellular compartmentalization of Drosophila neurons. *Neural Dev.* **2**, 7. doi:10.1186/1749-8104-2-7
Ryan, J. F. (2014). Did the ctenophore nervous system evolve independently? *Zoology (Jena)* **117**, 225-226. doi:10.1016/j.zool.2014.06.001
Ryan, J. F., Pang, K., Program, N. C. S., Mullikin, J. C., Martindale, M. Q. and Baxevanis, A. D. (2010). The homeodomain complement of the ctenophore Mnemiopsis leidyi suggests that Ctenophora and Porifera diverged prior to the ParaHoxozoa. *Evodevo* **1**, 9. doi:10.1186/2041-9139-1-9
Ryan, J. F., Pang, K., Schnitzler, C. E., Nguyen, A.-D., Moreland, R. T., Simmons, D. K., Koch, B. J., Francis, W. R., Havlak, P., Program, N. C. S. et al. (2013). The genome of the ctenophore Mnemiopsis leidyi and its implications for cell type evolution. *Science* **342**, 1242592. doi:10.1126/science.1242592
Sanchez-Huertas, C., Freixo, F., Viais, R., Lacasa, C., Soriano, E. and Luders, J. (2016). Non-centrosomal nucleation mediated by augmin organizes microtubules in post-mitotic neurons and controls axonal microtubule polarity. *Nat. Commun.* **7**, 12187. doi:10.1038/ncomms12187
Sarmiere, P. D., Weigle, C. M. and Tamkun, M. M. (2008). The Kv2.1 K+ channel targets to the axon initial segment of hippocampal and cortical neurons in culture and in situ. *BMC Neurosci.* **9**, 112. doi:10.1186/1471-2202-9-112
Satterlie, R. A. (1979). Central control of swimming in the cubomedusan jellyfish Carybdea rastonii. *J. Comp. Physiol.* **133**, 357-367. doi:10.1007/BF00661138
Satterlie, R. A. (2011). Do jellyfish have central nervous systems? *J. Exp. Biol.* **214**, 1215-1223. doi:10.1242/jeb.043687
Sebe-Pedros, A., Saudemont, B., Chomsky, E., Plessier, F., Mailhe, M. P., Renno, J., Loe-Mie, Y., Lifshitz, A., Mukamel, Z., Schmutz, S. et al. (2018). Cnidarian cell type diversity and regulation revealed by whole-organism single-cell RNA-Seq. *Cell* **173**, 1520-1534.e20. doi:10.1016/j.cell.2018.05.019
Shah, M. M., Migliore, M., Valencia, I., Cooper, E. C. and Brown, D. A. (2008). Functional significance of axonal Kv7 channels in hippocampal pyramidal neurons. *Proc. Natl. Acad. Sci. USA* **105**, 7869-7874. doi:10.1073/pnas.0802805105
Sharp, D. J., Yu, W., Ferhat, L., Kuriyama, R., Rueger, D. C. and Baas, P. W. (1997). Identification of a microtubule-associated motor protein essential for dendritic differentiation. *J. Cell Biol.* **138**, 833-843. doi:10.1083/jcb.138.4.833
Shiraishi-Yamaguchi, Y. and Furuichi, T. (2007). The Homer family proteins. *Genome Biol.* **8**, 206. doi:10.1186/gb-2007-8-2-206
Shu, X., Shaner, N. C., Yarbrough, C. A., Tsien, R. Y. and Remington, S. J. (2006). Novel chromophores and buried charges control color in mFruits. *Biochemistry* **45**, 9639-9647. doi:10.1021/bi060773l
Song, A.-H., Wang, D., Chen, G., Li, Y., Luo, J., Duan, S. and Poo, M. M. (2009). A selective filter for cytoplasmic transport at the axon initial segment. *Cell* **136**, 1148-1160. doi:10.1016/j.cell.2009.01.016
Srivastava, M., Begovic, E., Chapman, J., Putnam, N. H., Hellsten, U., Kawashima, T., Kuo, A., Mitros, T., Salamov, A., Carpenter, M. L. et al. (2008). The Trichoplax genome and the nature of placozoans. *Nature* **454**, 955-960. doi:10.1038/nature07191
Stefanik, D. J., Friedman, L. E. and Finnerty, J. R. (2013). Collecting, rearing, spawning and inducing regeneration of the starlet sea anemone, Nematostella vectensis. *Nat. Protoc.* **8**, 916-923. doi:10.1038/nprot.2013.044
Stepanova, T., Slemmer, J., Hoogenraad, C. C., Lansbergen, G., Dortland, B., De Zeeuw, C. I., Grosveld, F., van Cappellen, G., Akhmanova, A. and Galjart, N. (2003). Visualization of microtubule growth in cultured neurons via the use of EB3-GFP (end-binding protein 3-green fluorescent protein). *J. Neurosci.* **23**, 2655-2664. doi:10.1523/JNEUROSCI.23-07-02655.2003
Stiess, M., Maghelli, N., Kapitein, L. C., Gomis-Ruth, S., Wilsch-Brauninger, M., Hoogenraad, C. C., Tolic-Norrelykke, I. M. and Bradke, F. (2010). Axon extension occurs independently of centrosomal microtubule nucleation. *Science* **327**, 704-707. doi:10.1126/science.1182179
Stone, M. C., Roegiers, F. and Rolls, M. M. (2008). Microtubules have opposite orientation in axons and dendrites of Drosophila neurons. *Mol. Biol. Cell* **19**, 4122-4129. doi:10.1091/mbc.e07-10-1079
Strowbridge, B. W. (2009). Role of cortical feedback in regulating inhibitory microcircuits. *Ann. N. Y. Acad. Sci.* **1170**, 270-274. doi:10.1111/j.1749-6632.2009.04018.x
Tsien, R. Y. (1998). The green fluorescent protein. *Annu. Rev. Biochem.* **67**, 509-544. doi:10.1146/annurev.biochem.67.1.509
Watanabe, H., Fujisawa, T. and Holstein, T. W. (2009). Cnidarians and the evolutionary origin of the nervous system. *Dev. Growth Differ.* **51**, 167-183. doi:10.1111/j.1440-169X.2009.01103.x
Weiner, A. T., Seebold, D. Y., Torres-Gutierrez, P., Folker, C., Swope, R. D., Kothe, G. O., Stoltz, J. G., Zalenski, M. K., Kozlowski, C., Barbera, D. J. et al. (2020). Endosomal Wnt signaling proteins control microtubule nucleation in dendrites. *PLoS Biol.* **18**, e3000647. doi:10.1371/journal.pbio.3000647
Westfall, J. A. (1973). Ultrastructural evidence for a granule-containing sensory-motor-interneuron in Hydra littoralis. *J. Ultrastruct. Res.* **42**, 268-282. doi:10.1016/S0022-5320(73)90055-5
Winckler, B., Forscher, P. and Mellman, I. (1999). A diffusion barrier maintains distribution of membrane proteins in polarized neurons. *Nature* **397**, 698-701. doi:10.1038/17806
Wong, M. Y., Zhou, C., Shakiryanova, D., Lloyd, T. E., Deitcher, D. L. and Levitan, E. S. (2012). Neuropeptide delivery to synapses by long-range vesicle circulation and sporadic capture. *Cell* **148**, 1029-1038. doi:10.1016/j.cell.2011.12.036
Xiao, B., Tu, J. C., Petralia, R. S., Yuan, J. P., Doan, A., Breder, C. D., Ruggiero, A., Lanahan, A. A., Wenthold, R. J. and Worley, P. F. (1998). Homer regulates the association of group 1 metabotropic glutamate receptors with multivalent complexes of homer-related, synaptic proteins. *Neuron* **21**, 707-716. doi:10.1016/S0896-6273(00)80588-7
Yan, J., Chao, D. L., Toba, S., Koyasako, K., Yasunaga, T., Hirotsune, S. and Shen, K. (2013). Kinesin-1 regulates dendrite microtubule polarity in Caenorhabditis elegans. *Elife* **2**, e00133. doi:10.7554/eLife.00133.021
Yau, K. W., Schatzle, P., Tortosa, E., Pages, S., Holtmaat, A., Kapitein, L. C. and Hoogenraad, C. C. (2016). Dendrites In Vitro and In Vivo contain microtubules of opposite polarity and axon formation correlates with uniform plus-end-out microtubule orientation. *J. Neurosci.* **36**, 1071-1085. doi:10.1523/JNEUROSCI.2430-15.2016